


## RESEARCH ARTICLE

# Species variation in the cartilaginous endplate of the lumbar intervertebral disc

Yun-He Li<sup>1,2</sup> | Hai-Long Wu<sup>1,2</sup> | Zhen Li<sup>3</sup>  | Bin-Bin Li<sup>4</sup> | Man Zhu<sup>1,2</sup> | Di Chen<sup>5</sup> | Fei-Hong Ye<sup>6</sup> | Bin-Sheng Yu<sup>1,2,7</sup> | Yong-Can Huang<sup>1,2,7</sup> 

<sup>1</sup>Shenzhen Key Laboratory of Spine Surgery, Department of Spine Surgery, Peking University Shenzhen Hospital, Shenzhen, China

<sup>2</sup>Shenzhen Engineering Laboratory of Orthopaedic Regenerative Technologies, National & Local Joint Engineering Research Center of Orthopaedic Biomaterials, Peking University Shenzhen Hospital, Shenzhen, China

<sup>3</sup>AO Research Institute Davos, Davos, Switzerland

<sup>4</sup>Department of Human Anatomy & Histoembryology, Hangzhou Normal University, Hangzhou, China

<sup>5</sup>Research Center for Computer-aided Drug Discovery, Shenzhen Institute of Advanced Technology, Chinese Academy of Sciences, Shenzhen, China

<sup>6</sup>Hangzhou Zhigu Research Center for Tissue Engineering and Regenerative Medicine, Hangzhou, China

<sup>7</sup>Institute of Orthopaedics, Peking University Shenzhen Hospital, Shenzhen Peking University-The Hong Kong University of Science and Technology Medical Center, Shenzhen, China

## Correspondence

Fei-Hong Ye, Hangzhou Zhigu Research Center for Tissue Engineering and Regenerative Medicine, Hangzhou, China. Email: [yefeihong@honylbiomed.com](mailto:yefeihong@honylbiomed.com)

Bin-Sheng Yu and Yong-Can Huang, Department of Spine Surgery, Peking University Shenzhen Hospital, No. 1120, Lianhua Road, Shenzhen 518036, China. Email: [hpyubinsheng@hotmail.com](mailto:hpyubinsheng@hotmail.com); [y.c.huang@connect.hku.hk](mailto:y.c.huang@connect.hku.hk)

## Abstract

**Backgrounds:** Cartilaginous endplate (CEP) plays an essential role in intervertebral disc (IVD) health and disease. The aim was to compare the CEP structure of lumbar IVD and to reveal the detailed pattern of integration between the CEP and bony endplate (BEP) from different species.

**Methods:** A total of 34 IVDs (5 human, 5 goat, 8 pig, 8 rabbit, and 8 rat IVDs) were collected, fixed and midsagittally cut; in each IVD, one-half was used for histological staining to observe the CEP morphology, and the other half was used for scanning electron microscopy (SEM) analysis to measure the diameters and distributions of collagen fibers in the central and peripheral CEP areas and to observe the pattern of CEP-BEP integration from different species.

**Results:** The human, pig, goat, and rabbit IVDs had the typical BEP-CEP structure, but the rat CEP was directly connected with the growth plate. Human CEP was the thickest ( $896.95 \pm 87.71 \mu\text{m}$ ) among these species, followed by pig, goat, rat, and rabbit CEPs. Additionally, the mean cellular density of the rabbit CEP was the highest, which was  $930 \pm 202$  per  $\text{mm}^2$ , followed by the rat, goat, pig, and human CEPs. In all the species, the collagen fiber diameter in the peripheral area was much bigger than that in the central area. The collagen fiber diameters of CEP from the human, pig, goat, and rat were distributed between 35 nm and 65 nm. The BEP and CEP were connected by the collagen from the CEP, aggregating into bundles or cross links with each other to form a network, and anchored to BEP.

**Conclusions:** Significant differences in the thickness, cellular density, and collagen characterization of CEPs from different species were demonstrated; the integration of BEP-CEP in humans, pigs, goats, and rabbits was mainly achieved by the collagen bundles anchoring system, while the typical BEP-CEP interface did not exist in rats.

## KEYWORDS

bony endplate, cartilaginous endplate, intervertebral disc, species variation

Yun-He Li and Hai-Long Wu contributed equally to this work.

This is an open access article under the terms of the [Creative Commons Attribution-NonCommercial-NoDerivs](https://creativecommons.org/licenses/by-nc-nd/4.0/) License, which permits use and distribution in any medium, provided the original work is properly cited, the use is non-commercial and no modifications or adaptations are made.

© 2022 The Authors. *JOR Spine* published by Wiley Periodicals LLC on behalf of Orthopaedic Research Society.

## 1 | INTRODUCTION

Intervertebral disc (IVD) repair and regeneration have been regarded as one of the main strategies to treat IVD degenerative diseases, aiming at pain relief, neurological improvement, and biomechanical restoration.<sup>1,2</sup> In the past decades, the central nucleus pulposus and the peripheral annulus fibrosus of IVDs have been investigated in depth, with the focus of studies ranging from degenerative mechanisms to the development of reparative approaches. Several important objectives have been achieved using various biological approaches: (a) rejuvenation of resident disc cells, (b) augmentation of disc components and extracellular matrix, (c) reestablishment of disc microenvironment and homeostasis, and (d) reconstruction of IVD structure and kinematics.<sup>3-5</sup> However, most of these functions have been validated in the nucleus pulposus or annulus fibrosus, while another important structure of IVD—the endplates—have been typically neglected.

The endplates are located at the cranial and caudal ends of each IVD and sandwich the central nucleus pulposus and the peripheral annulus fibrosus. In humans, normal endplates are composed of an outer cortical bone (the bony endplate [BEP]) and an inner cartilaginous layer (the cartilaginous endplate [CEP]). Structurally, the endplates prevent the bulging of the disc into the adjacent vertebral bodies<sup>6</sup> and provide secure anchorage for the insertion nodes of the disc to ensure structural integration.<sup>7,8</sup> As a mechanical interface, the other function of endplates is to disperse the compressive loading experienced by the vertebra-disc complex.<sup>9</sup> The CEP is also the predominant regulator for nutrient transportation to the IVD; the nutrient supply to most of the disc cells has to pass through the CEP by diffusion.<sup>4,10</sup> The average diffusivities of glucose and lactate in human CEPs are  $2.68 \times 10^{-7}$  and  $4.52 \times 10^{-7}$  cm<sup>2</sup>/s with the highest value in the central region;<sup>11</sup> the biochemical composition of the CEP affects the diffusivity, thus regulating the disc cells survival and function.<sup>12</sup> Therefore, the CEP plays a critical role in maintaining the health and function of IVD and in the success of biological therapies.

At present, several animal models such as mice,<sup>13</sup> rats,<sup>14</sup> rabbits,<sup>15</sup> pigs, goats,<sup>16-18</sup> dogs, and nonhuman primates<sup>19,20</sup> have been extensively used for studying the reparative treatments to IVD-related disorders; additionally, bovine coccygeal IVD has been frequently utilized as an organ culture model *in vitro*.<sup>21,22</sup> In these species, the rodents, rabbits, pigs, goats and dogs had the structure of vertebral growth plates that persisted through adulthood, and this structure was not seen in adult humans.<sup>23</sup> In some studies that used rodents as an animal model, the growth plate was mistakenly identified as the CEP;<sup>24</sup> it thus became meaningless to extrapolate the results found in the animals to the human CEP. Previous studies have mentioned that the endplates from different species possess different structures,<sup>23,25</sup> but currently, no studies histologically characterize and compare the CEP from the lumbar IVD of rodents, rabbits, goats, pigs and humans and directly compare the central and peripheral CEP from the same species.

The BEP and CEP are not simply mixed to act as the structural transition between the hard vertebral bodies and the soft IVD; a sophisticated structure is necessary to keep the integration of BEP and CEP, as well as the biomechanical and nutritional functions. Using

a light microscope, a previous study found that the anchorage of the annulus in CEP was achieved by the annular fiber subbundles separated by the CEP matrix.<sup>26</sup> Nevertheless, the detailed pattern of integration of CEP and BEP from different species is far from well understood.

In this study, using the lumbar discs obtained from rats, rabbits, goats, pigs and humans, we described and compared the morphologies of the central and peripheral CEP from different species; in particular, we focused on the integration mechanism between the CEP and BEP, with the aim of better understanding the species variation of lumbar CEP.

## 2 | MATERIALS AND METHODS

### 2.1 | Collection of lumbar IVD specimens

Human lumbar IVDs (L1–L5) with 1–2 cm of adjacent vertebral bodies were obtained from a 24-year-old male cadaveric organ donor from the Department of Human Anatomy & Histoembryology, Hangzhou Normal University, and ethical approval was obtained. Goat IVDs (L2–L6) were obtained from 9- to 12-month-old male Hainan Dong goats from our previous study.<sup>27</sup> Pig IVDs (L2–L6) were obtained from 2- to 3-month-old male Bama miniature pigs (weight 8–10 kg), rabbit IVDs (L3–L7) were obtained from 5- to 6-month-old male New Zealand white rabbits (weight 5–6 kg) and rat IVDs (L2–L5) were obtained from 2- to 3-month-old male SD rats (weight 330–360 g). The experiments in this study were approved by the Laboratory Animal Welfare Ethics Committee of Shenzhen PKU-HKUST Medical Center.

After removing the surrounding ligaments and muscles, five human IVDs, eight pig IVDs, five goat IVDs, eight rabbit IVDs, and eight rat IVDs were obtained and fixed in 10% neutral formalin solution for 2–7 days. All IVDs were midsagittally cut using a band saw (EXAKT312, Norderstedt, Germany); one-half of the IVD was used for histological staining, and the other half was used for scanning electron microscopy (SEM) analysis.

### 2.2 | Histological staining and analysis

The IVDs were decalcified, dehydrated and embedded in paraffin wax and then cut into 5 μm-thick sections for hematoxylin and eosin (HE) and toluidine blue staining. The morphological differences of the CEP from different species were observed using a microscope (Leica DM4B, Germany). The CEP was divided into central and peripheral areas; the area of the CEP adjacent to the nucleus pulposus was defined as the central area and the area of the CEP adjacent to the annulus fibrosus (including the inner annulus fibrosus and the outer annulus fibrosus) was defined as the peripheral area.

The thickness and cellular density of the central and peripheral regions of the CEP in different species were calculated. For the CEP thickness measurement, at least five images of 200× CEP from each species (except the human CEP, which used 50× images since it was thicker than that of other species) were randomly selected after toluidine blue staining; Image J was used to measure the CEP thickness by two individuals, and each image was measured three times. The CEP

thickness was the average value of multiple measurements. For the CEP cellular density measurement, at least five images of 200× CEP from each species were randomly selected after H&E staining, and two individuals calculated the number of chondrocytes in the CEP using the following formula: The cellular density = the number of chondrocytes/calculated area. Because of the fresh-frozen and other processing procedures, some empty chondrocyte lacunae were seen in the human IVDs and they were also included for the measurement of cellular density.

## 2.3 | SEM analysis

The other half of the IVDs used for the SEM analysis were dehydrated by gradient ethanol-90% ethanol for 1 h and anhydrous ethanol for another hour—followed by critical point drying. After gold sputtering,

the specimens were placed in the SEM (MIRA3, TESCAN, Czech) for microstructure and collagen observation. For the collagen fiber diameter measurement, four 50 000× SEM images were randomly selected and two individuals used Image J to measure the collagen fiber diameter. Twenty collagen fibers were randomly calculated for each image. The distributions of collagen fiber diameters in the central and peripheral areas of the CEP in different species and the CEP-BEP interface were observed.

## 2.4 | Statistical analysis

All data were presented as mean ± SD. One-way ANOVA or the non-parametric Kruskal-Wallis test was used to determine the significance of differences between the different groups. The statistical significance was set at  $p < 0.05$ .

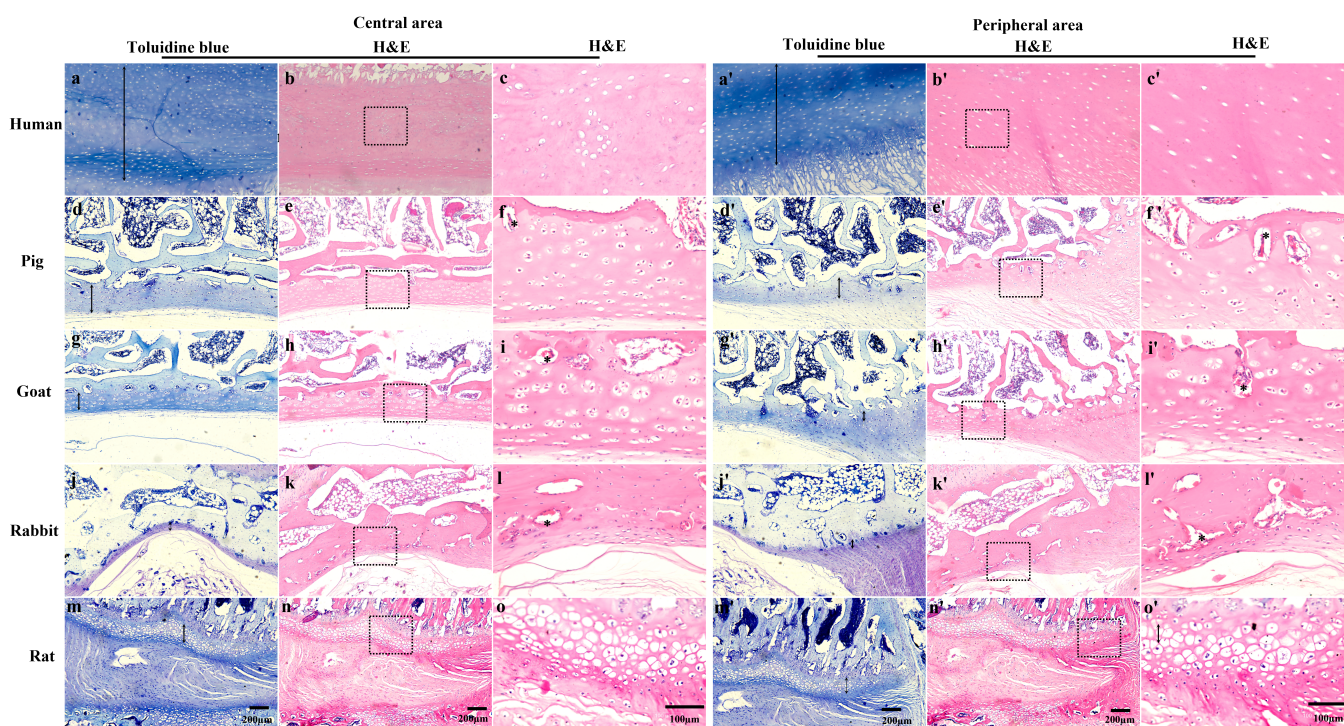


**FIGURE 1** H&E and toluidine blue staining of CEP from different species (a–c and a'–c', the central and peripheral area of human CEP; d–f and d'–f', the central and peripheral area of pig CEP; g–i and g'–i', the central and peripheral area of goat CEP; j–l and j'–l', the central and peripheral area of rabbit CEP; m–o and m'–o', the central and peripheral area of rat CEP; double-headed arrow, CEP; \*vascular channels)

**TABLE 1** The thickness and cellular density of CEP from different species ( $\bar{X} \pm SD$ )

	Whole area		Central area		Peripheral area	
	Thickness ( $\mu\text{m}$ )	Cellular density (per $\text{mm}^2$ )	Thickness ( $\mu\text{m}$ )	Cellular density (per $\text{mm}^2$ )	Thickness ( $\mu\text{m}$ )	Cellular density (per $\text{mm}^2$ )
Human	896.95 ± 87.71	231 ± 44	855.58 ± 24.37 <sup>##</sup>	259 ± 31 <sup>##</sup>	938.31 ± 108.44	203 ± 36
Pig	292.29 ± 26.29 <sup>**</sup>	505 ± 144 <sup>**</sup>	304.80 ± 17.47 <sup>##</sup>	605 ± 132 <sup>##</sup>	279.24 ± 27.72	409 ± 67
Goat	267.169 ± 30.11 <sup>**</sup>	622 ± 83 <sup>**</sup>	267.70 ± 26.01	684 ± 60 <sup>##</sup>	266.64 ± 34.91	561 ± 50
Rabbit	71.61 ± 10.57 <sup>**</sup>	930 ± 202 <sup>**</sup>	69.41 ± 9.79	991 ± 200	73.81 ± 11.27	868 ± 192
Rat	249.03 ± 54.50 <sup>**</sup>	683 ± 118 <sup>**</sup>	288.96 ± 49.00 <sup>##</sup>	603 ± 93 <sup>##</sup>	209.10 ± 18.16	762 ± 81

Note: The whole CEP in other species compared with humans, <sup>\*\*</sup> $p < 0.01$ . The central and peripheral areas of the CEP comparisons for each species, <sup>##</sup> $p < 0.01$ .

### 3 | RESULTS

#### 3.1 | Species variation in the morphology and cellular density of CEP

As illustrated in Figure 1a-c, the central region of human CEP was composed of a toluidine blue-positive matrix (such as proteoglycan) and 10–15 layers of chondrocytes; the distribution of chondrocytes in the peripheral zone was more scattered than that in the central zone.

The distribution of matrix and chondrocytes in pig and goat CEPs were similar; cells near nucleus pulposus were more densely distributed than those near the BEP and cells in the peripheral areas were arranged more disordered (Figure 1d-i'). The rabbit had the thinnest CEP and the curvature of the CEP in the central region was the largest among these species (Figure 1j-l); the boundary between the endplate and the annulus fibrosus in the peripheral region was not particularly obvious (Figure 1j'-l'). The structure of rat endplates was the most different from that of other species. Because of the absence of BEP, the

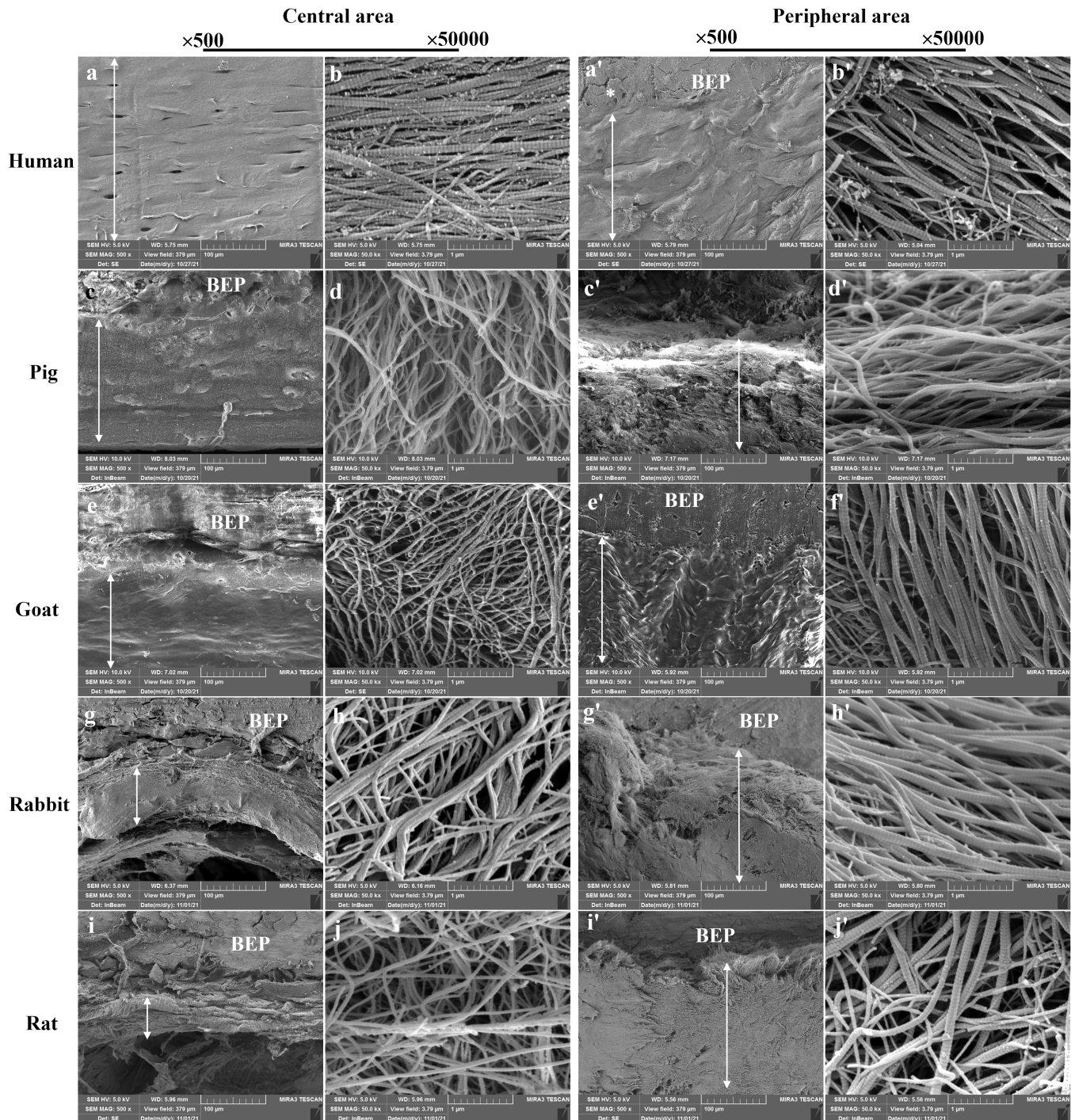


**FIGURE 2** Scanning electron microscopy (SEM) images of CEP from different species (a-b and a'-b', the central and peripheral area of human CEP; c-d and c'-d', the central and peripheral area of pig CEP; e-f and e'-f', the central and peripheral area of goat CEP; g-h and g'-h', the central and peripheral area of rabbit CEP; i-j and i'-j', the central and peripheral area of rat CEP; double-headed arrow, CEP)

CEP was directly connected to its growth plate (Figure 1m-o); the central area was the thickest, and the closer it was to the periphery, the thinner the CEP. Additionally, a large number of tightly packed chondrocytes were arranged in rat CEP.

As shown in Table 1, the average thickness of human CEP was the largest ( $896.95 \pm 87.71 \mu\text{m}$ ), while that of rabbit CEP was the smallest ( $71.61 \pm 10.57 \mu\text{m}$ ). The peripheral area of the human CEP was thicker than the central area, while in the pig and rat CEPs, it was the opposite ( $p < 0.01$ ). The average cellular density of the rabbit CEP was the largest ( $930 \pm 202 \text{ per mm}^2$ ), while that in humans was the smallest, with a value of  $231 \pm 44 \text{ per mm}^2$ . The cellular density in all the other species was greater than that in humans ( $p < 0.01$ ). Furthermore, there was a significant difference in cellular density between the central and peripheral regions of CEP in humans, pigs, goats and rats ( $p < 0.01$ ).

### 3.2 | Collagen features and distribution in the CEP in different species

As illustrated in Figure 2, the collagen in the central and peripheral regions of the human CEP were arranged in parallel and the collagen gap was small. The collagen in the pig CEP was like that of goats. In the central area of the pig and goat CEPs, the collagen was intertwined and arranged neatly in parallel in the peripheral area; the collagen gap was larger than that in the human CEP. Notably, collagen in the central area of rabbit CEP aggregated into bundles and was cross-linked, and the collagen fiber diameter was significantly larger than that in human CEP. The arrangement of collagen in the rat CEP was the most disordered and interwoven in a network, and the collagen fiber diameter in the peripheral area was significantly larger than that in the central area.

As shown in Table 2, the mean collagen fiber diameter of the CEP in these species ranged from 51.69 to 76.16 nm; the value of rat CEP was the largest, while that of goats was smallest. In pigs, goats, rabbits and rats, the diameter of the collagen fibers in the peripheral area was much larger than that in the central area of the CEP ( $p < 0.05$ ). As

**TABLE 2** The collagen fiber diameter of CEP from different species ( $\bar{X} \pm \text{SD}$ )

	Average collagen fiber diameter (nm)	Collagen fiber diameter of central area (nm)	Collagen fiber diameter of peripheral area (nm)
Human	$62.38 \pm 25.18$	$57.18 \pm 17.11$	$67.58 \pm 30.48$
Pig	$60.49 \pm 21.86$	$57.53 \pm 24.10^\#$	$63.46 \pm 19.05$
Goat	$51.69 \pm 13.34^{**}$	$47.83 \pm 11.84^{##}$	$55.56 \pm 17.40$
Rabbit	$68.94 \pm 21.86^{**}$	$60.83 \pm 18.64^{##}$	$77.06 \pm 21.92$
Rat	$76.16 \pm 43.83$	$45.06 \pm 8.98^{##}$	$107.25 \pm 42.74$

Note: The whole CEP in other species compared with humans,  $^{**}p < 0.01$ . The central and peripheral areas of the CEP comparisons for each species,  $^\#p < 0.05$ ;  $^{##}p < 0.01$ .

illustrated in Figure 3, the collagen fiber diameters of human, pig, goat and rat CEPs were distributed between 35 and 65 nm, while rabbit was distributed between 60 and 80 nm. In the central area, the collagen fiber diameters of human, pig, goat, rabbit, and rat CEPs were mainly distributed between the ranges 40–80, 30–60 nm, 40–55 nm, 40–65 nm, and 35–50 nm, respectively; in the peripheral area, the collagen fiber diameters of CEP in humans and rats had two main intervals of distribution, which were 40–60 nm and 80–90 nm in humans, and 60–80 nm and 140–155 nm in rats.

### 3.3 | The interface between CEP and BEP in different species

Since there was no typical BEP structure in rats, the CEP-BEP interface could not be observed by SEM. As shown in Figure 4, the connection of CEP and BEP depended mainly on the collagen fibers emitting from the CEP, extending to the BEP and anchoring in the internal area of the BEP. In the central area of the human, pig, and goat CEPs, the collagen was aggregated into bundles and inserted into the BEP structure directly; the collagen in the central area of rabbit CEP was cross linked and aggregated into a network near the bone area, and the network structure and collagen fibers directly penetrated the BEP. Similarly, in the peripheral area of human, pig, and goat CEPs, the collagen was directly anchored in the BEP after aggregating into bundles; also, a small number of collagen fibers in the CEP directly entered the BEP and crosslinked with other collagens. The collagen fibers in the peripheral region of the rabbit CEP were like those in its central region; they aggregated into bundles and connected with each other to form a network and penetrated into the BEP. Thus, in view of the SEM results, no significant difference was found in the interface between CEP and BEP in different species.

## 4 | DISCUSSION

To the best of our knowledge, this study was the first to compare the structural differences of CEPs from different species. We found that the human lumbar disc had the thickest CEP and the rabbit had the thinnest one, but the rabbit CEP possessed the largest cellular density, while that of human CEP was the smallest. It was further determined that rabbits and rats had much larger collagen fiber diameter than humans, goats and pigs; additionally, in all these species, the collagen fiber diameter of CEP in the peripheral area was much larger than that in the central area. In the absence of BEP, there was no typical BEP-CEP interface in rats, and the pattern of BEP-CEP integration in other species was quite similar. In view of BEP-CEP integration, cellular density, collagen fiber diameter and distribution, the CEP from pig and goat were similar to human CEP.

Several kinds of animals, such as mice, rats, rabbits, pigs, goats, sheep, cows and nonhuman primates, have been utilized as highly valuable tools to investigate the biological therapies for degenerated IVDS.<sup>28,29</sup> Endplate injury has been found to be a feasible method to

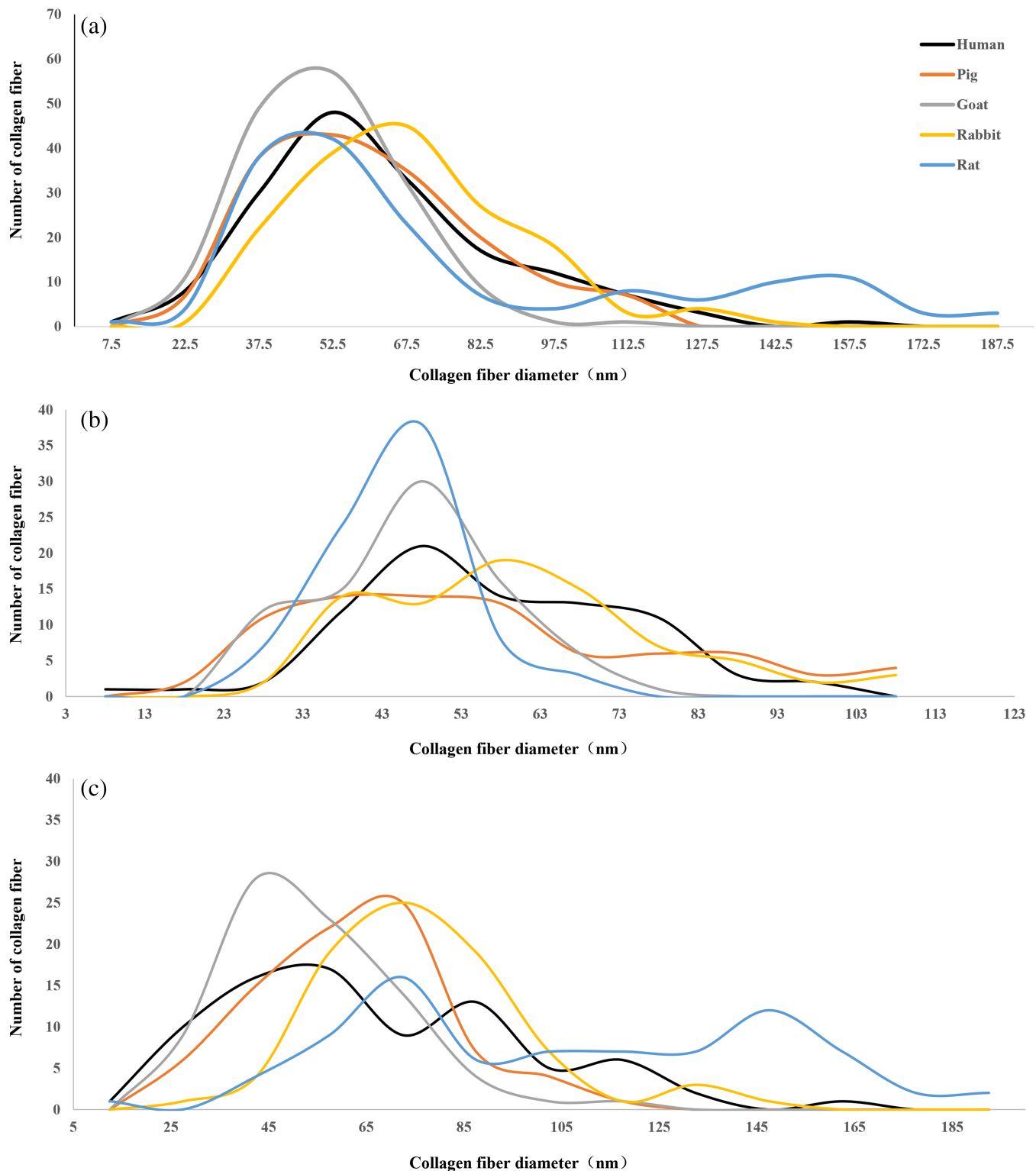


**FIGURE 3** Distribution of collagen fiber diameter of CEP from different species (a, distribution of collagen fiber diameter of CEP in different species (nm); b, Distribution of collagen fiber diameter in central area of CEP from different species (nm); c, Distribution of collagen fiber diameter in peripheral area of CEP from different species [nm])

induce IVD degeneration in animals. By injecting ping yangmycin into the subchondral bone adjacent to the IVD of rhesus monkeys, the significant reductions of the mean T1 $\rho$  values of nucleus pulposus and the disc height index were recorded; similar induced degenerative

changes could be found in rabbits.<sup>30,31</sup> Also, perforating the endplates to nucleus pulposus could cause IVD degeneration in pigs.<sup>32</sup> Further, the cement injections have been used to block the endplate nutrition pathway in goat lumbar IVD; degenerative changes in the disc cells

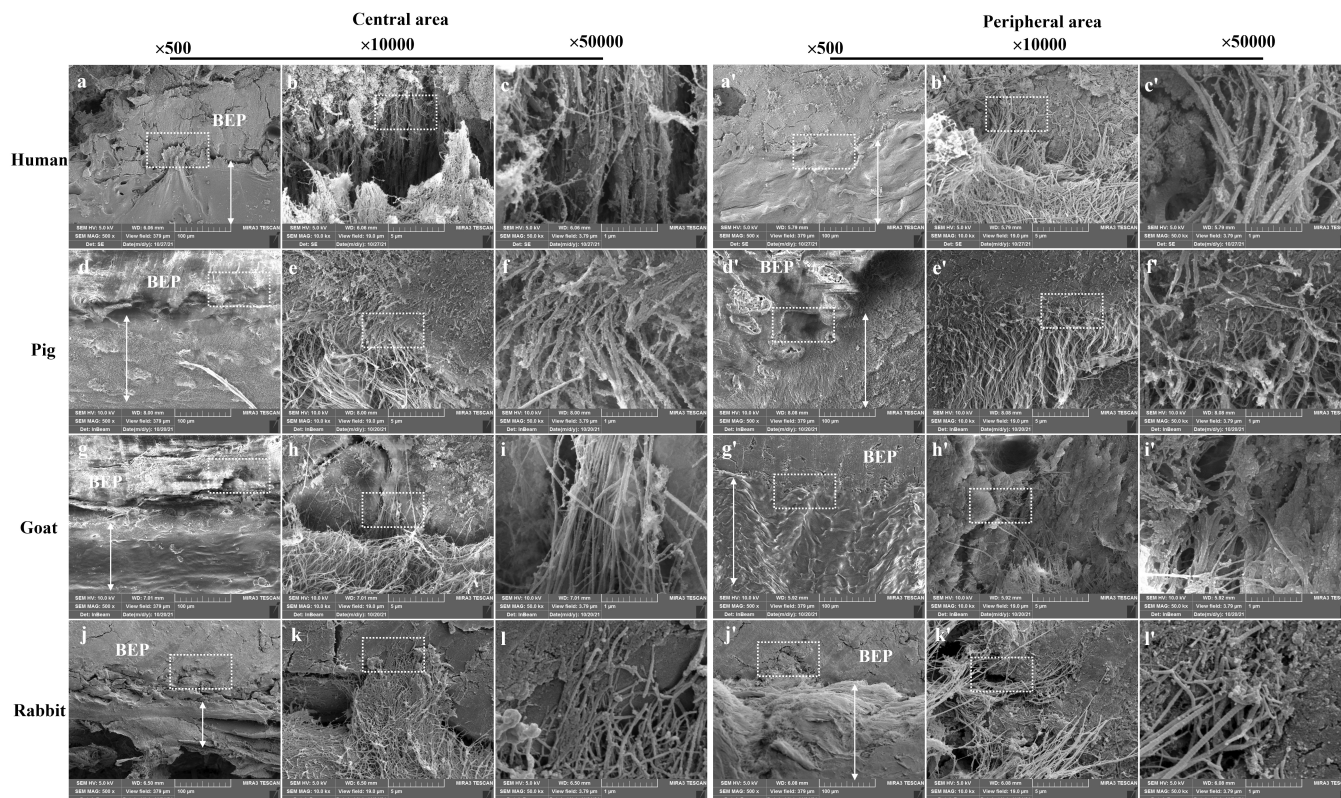


**FIGURE 4** Scanning electron microscopy (SEM) images of the interface between CEP and BEP from different species (a-c and a'-c', the central and peripheral area of human CEP; d-f and d'-f', the central and peripheral area of pig CEP; g-i and g'-i', the central and peripheral area of goat CEP; j-l and j'-l' the central and peripheral area of rabbit CEP) (double-headed arrow, CEP)

and matrix, as well as the ingrowth of vessels in the CEP, could be detected.<sup>33</sup> Nevertheless, injecting cement adjacent to endplates for up to 70 weeks did not induce obvious degeneration in dog IVD.<sup>34</sup> Recently, it was reported that a single impact injury without structural impairment to the EP was able to cause IVD degeneration in rats.<sup>35</sup> Therefore, it remains controversial whether blocking the endplate pathway can lead to successful IVD degeneration. This controversy may be attributed to endplate variations in different species. At present, many researchers used mice or rats to repair the degenerated IVD, but if the research aim is to repair the endplates or even the IVD nutrition, the mouse or rat model should be inappropriate according to the findings in this study.

In previous studies led by Dr Jill Urban, it was determined that the mean cellular density of the human IVDs as a whole was about 6000 cells/mm<sup>3</sup> and that there was a decline in cellularity from the CEP (about 15 000 cells/mm<sup>3</sup>) towards the central nucleus.<sup>36</sup> In addition, the endplate architecture has been found to have an important role in the IVD cellularity.<sup>37</sup> In our study, after cross-species comparison, a decrease in the CEP cellular density was seen when the CEP thickness increased. As we only calculated the CEP cell density with a semiquantitative method based on the histological images, it would be much better to measure the CEP cell density from different species using the optimized protocols,<sup>38</sup> which would be very meaningful to determine whether the cell density in CEP influences that in the whole IVD.

As the main component of the extracellular matrix in the IVD, collagen was organized into various fiber networks, providing the tensile strength required for specific functions.<sup>39</sup> Collagen constituted a highly specialized superfamily with at least 28 genetically distinct types, nine of which could be found in IVD: types I, II, III, V, VI, IX, XI, XII, and XIV.<sup>40,41</sup> The collagen network in CEPs was mainly formed by collagen type II, which not only maintained the stability of the CEP, but also prevented NP bulge, dispersed the tension of nucleus pulposus, reduced water loss and prevented the nucleus pulposus from protruding towards vertebral bodies.<sup>42</sup> In this study, collagen aggregation and entanglement in the CEP of rabbits and rats were more pronounced than in the CEP of humans, goats and pigs. Besides collagen, elastin was the other important component in the IVD matrix, which played an important role in reinforcing the integrity of collagen lamellae and supporting collagen recovery after deformation.<sup>43</sup> However, the detailed composition and types of collagen in these different species remain unclear.

Soft tissue-to-bone transitions are complex junctions that connect multiple tissue types and are critical for musculoskeletal function. The transitions of ligament-to-bone,<sup>44</sup> tendon-to-bone,<sup>45</sup> articular cartilage-to-bone interfaces<sup>46</sup> have been deeply studied. Nevertheless, few studies have focused on the interface between CEP and BEP. The osteochondral tissue was composed of articular cartilage, calcified cartilage layer and subchondral bone; the gradient variations in the number and

orientation of cells, and orientation of ECM collagen fibers have been seen.<sup>47</sup> The articular cartilage thus could be divided into three areas: the superficial tangential zone, the transition/middle zone and the radial/deep zone.<sup>47</sup> In the superficial zone, the collagen fibers were highly organized and arranged parallel to the articular surface to resist friction and shear force generated by joint motion;<sup>47,48</sup> in the transition zone, the collagen fibers were inclined or perpendicular to the tidal mark, which lied between the calcified and noncalcified cartilage layers;<sup>48</sup> in the deep zone, the collagen fibers had the largest diameter and were arranged in parallel with cells and perpendicular to the articular surface, which could strengthen the anchoring bond between the cartilage and bone.<sup>49,50</sup> This study found that the collagen fiber diameters of CEP in different species were different; therefore, the anchoring ability of CEP and BEP may be different in these species. A fiber connection was also found between the CEP (both the central and peripheral areas) and the BEP in different species; the collagen fibers in the CEP were directly anchored on the BEP after aggregating into bundles. Further study will be needed to determine the transition between the CEP and BEP, especially the force transmission.

This study compared the structural differences of CEP from different species for the first time; however, we should acknowledge that some limitations exist. In this work, all the IVDs specimens were obtained from the young animals with sexual maturity. Unlike the adult humans, the structure of vertebral growth plates persisted through the adulthood of these experimental animals,<sup>23</sup> it was thus not easy to choose the animals with skeletal maturity for cross-species comparison. Therefore, in this study, it remains unclear how the age of the animals influences the thickness, cellular density and collagen characterization of CEPs, as well as the integration of BEP-CEP. Second, it was recently reported that fluid transport varied by spine level and transport declined from cranial to caudal along the lumbar spine,<sup>51</sup> which may relate to the difference in CEP diffusion capacity in different segments. Hence, it is meaningful to know how the discal levels affect the anatomical structure of the CEP. Third, a quantitative analysis of the cells and extracellular matrix composition in the central and peripheral areas of the CEP from these species is needed. Fourth, it is still unclear whether the formalin fixation affects the collagen fiber diameter. Last but not the least, for the CEP-BEP interface, it is extremely necessary to further analyze the composition, mechanical properties, microstructure and physiological metabolism of this interface among different species to better distinguish the similarities and differences of this interface among different species and to take these differences into account during the design and fabrication of osteochondral repair strategies for IVD regeneration.

## 5 | CONCLUSION

In this study, species variation in the CEP of lumbar IVDs was determined based on histology and SEM analysis. Significant differences in the thickness, cellular density and collagen fiber diameter and distribution of CEPs from different species were recorded; in all these species, the collagen fiber diameter of CEP in the peripheral area was much bigger than that in the central area. In the absence of BEP, there

was no typical BEP-CEP interface in rats, and the integration of BEP-CEP in humans, pigs, goats and rabbits was mainly achieved by the collagen bundles anchoring system. In view of the BEP-CEP integration, the cellular density, collagen characterization, the pig and goat CEPs were similar to human CEP. This study suggested that we should take full account of these differences in different animal models when investigating the physiological changes of the CEP or CEP-based repair strategies for IVD degeneration.

## AUTHOR CONTRIBUTIONS

All the authors have read and approve the final manuscript for submission. Yun-He Li, Hai-Long Wu, Bin-Bin Li, and Man Zhu contributed to data acquisition, data interpretation, manuscript drafting and statistical analysis. Zhen Li and Di Chen contributed to data interpretation, manuscript editing. Fei-Hong Ye and Bin-Sheng Yu contributed to conception and design, data acquisition and obtaining funding. Yong-Can Huang contributed to conception and design, obtaining funding, data interpretation, manuscript drafting, and critical revisions.

## ACKNOWLEDGMENTS

This work was supported by the National Natural Science Foundation of China (No. 81702171 & No. 82030067), the Guangdong Basic and Applied Basic Research Foundation (No. 2021A1515220086 & No. 2022A1515011536), the Shenzhen Double Chain Project for Innovation and Development Industry supported by the Bureau of Industry and Information Technology of Shenzhen (No. 201806081018272960) and the Shenzhen Science and Technology Programs (No. JCYJ20190809182213535 & No. GJHZ20210705142543019).

## CONFLICT OF INTEREST

The authors report no conflicts of interest.

## DATA AVAILABILITY STATEMENT

The data used to support the findings of this study are included within the article.

## ORCID

Zhen Li  <https://orcid.org/0000-0002-9754-6389>

Yong-Can Huang  <https://orcid.org/0000-0001-8548-8233>

## REFERENCES

- Huang YC, Hu Y, Li Z, Luk KDK. Biomaterials for intervertebral disc regeneration: current status and looming challenges. *J Tissue Eng Regen Med.* 2018;12(11):2188-2202.
- Huang YC, Leung VY, Lu WW, Luk KD. The effects of microenvironment in mesenchymal stem cell-based regeneration of intervertebral disc. *Spine J.* 2013;13(3):352-362.
- Binch ALA, Fitzgerald JC, Growney EA, Barry F. Cell-based strategies for IVD repair: clinical progress and translational obstacles. *Nat Rev Rheumatol.* 2021;17(3):158-175.
- Huang YC, Urban JP, Luk KD. Intervertebral disc regeneration: do nutrients lead the way? *Nat Rev Rheumatol.* 2014;10(9):561-566.
- Lyu FJ, Cheung KM, Zheng Z, Wang H, Sakai D, Leung VY. IVD progenitor cells: a new horizon for understanding disc homeostasis and repair. *Nat Rev Rheumatol.* 2019;15(2):102-112.



6. Roberts S, Urban JP, Evans H, Eisenstein SM. Transport properties of the human cartilage endplate in relation to its composition and calcification. *Spine (Phila pa 1976)*. 1996;21(4):415-420.
7. Wade KR, Robertson PA, Broom ND. A fresh look at the nucleus-endplate region: new evidence for significant structural integration. *Eur Spine J*. 2011;20(8):1225-1232.
8. Wade KR, Robertson PA, Broom ND. On how nucleus-endplate integration is achieved at the fibrillar level in the ovine lumbar disc. *J Anat*. 2012;221(1):39-46.
9. Ferguson SJ, Steffen T. Biomechanics of the aging spine. *Eur Spine J*. 2003;12(Suppl 2):S97-S103.
10. Urban JP, Smith S, Fairbank JC. Nutrition of the intervertebral disc. *Spine (Phila pa 1976)*. 2004;29(23):2700-2709.
11. Wu Y, Cisewski SE, Wegner N, et al. Region and strain-dependent diffusivities of glucose and lactate in healthy human cartilage endplate. *J Biomech*. 2016;49(13):2756-2762.
12. Wong J, Sampson SL, Bell-Briones H, et al. Nutrient supply and nucleus pulposus cell function: effects of the transport properties of the cartilage endplate and potential implications for intradiscal biologic therapy. *Osteoarthr Cartil*. 2019;27(6):956-964.
13. Yang F, Leung VY, Luk KD, Chan D, Cheung KM. Mesenchymal stem cells arrest intervertebral disc degeneration through chondrocytic differentiation and stimulation of endogenous cells. *Mol Ther*. 2009;17(11):1959-1966.
14. Crevensten G, Walsh AJL, Ananthakrishnan D, et al. Intervertebral disc cell therapy for regeneration: mesenchymal stem cell implantation in rat intervertebral discs. *Ann Biomed Eng*. 2004;32(3):430-434.
15. Sakai D, Mochida J, Yamamoto Y, et al. Transplantation of mesenchymal stem cells embedded in Atelocollagen gel to the intervertebral disc: a potential therapeutic model for disc degeneration. *Biomaterials*. 2003;24(20):3531-3541.
16. Zhang Y, Drapeau S, An HS, Markova D, Lenart BA, Anderson DG. Histological features of the degenerating intervertebral disc in a goat disc-injury model. *Spine (Phila pa 1976)*. 2011;36(19):1519-1527.
17. Smit TH. The use of a quadruped as an in vivo model for the study of the spine - biomechanical considerations. *Eur Spine J*. 2002;11(2):137-144.
18. Verlaan JJ, Oner FC, Slootweg PJ, Verbout AJ, Dhert WJ. Histologic changes after vertebroplasty. *J Bone Joint Surg Am*. 2004;86(6):1230-1238.
19. Luk KD, Ruan DK, Chow DH, Leong JC. Intervertebral disc autografting in a bipedal animal model. *Clin Orthop Relat Res*. 1997;337:13-26.
20. Luk KD, Ruan DK, Lu DS, Fei ZQ. Fresh frozen intervertebral disc allografting in a bipedal animal model. *Spine (Phila pa 1976)*. 2003;28(9):864-869.
21. Chen JX, Li YH, Wen J, Li Z, Yu BS, Huang YC. Annular defects impair the mechanical stability of the intervertebral disc. *Global Spine J*. 2021;21925682211006061.
22. Cui S, Zhou Z, Chen X, et al. Transcriptional profiling of intervertebral disc in a post-traumatic early degeneration organ culture model. *JOR Spine*. 2021;4(3):e1146.
23. Zhang Y, Lenart BA, Lee JK, et al. Histological features of endplates of the mammalian spine: from mice to men. *Spine (Phila pa 1976)*. 2014;39(5):E312-E317.
24. Li H, Yan JZ, Chen YJ, Kang WB, Huang JX. Non-invasive quantification of age-related changes in the vertebral endplate in rats using in vivo DCE-MRI. *J Orthop Surg Res*. 2017;12(1):169.
25. Lakstins K, Arnold L, Gunsch G, Khan S, Moore S, Purmessur D. Characterization of bovine and canine animal model cartilage endplates and comparison to human cartilage endplate structure, matrix composition, and cell phenotype. *JOR Spine*. 2020;3(4):e1116.
26. Rodrigues SA, Wade KR, Thambyah A, Broom ND. Micromechanics of annulus-end plate integration in the intervertebral disc. *Spine J*. 2012;12(2):143-150.
27. Xiao J, Huang YC, Lam SK, Luk KD. Surgical technique for lumbar intervertebral disc transplantation in a goat model. *Eur Spine J*. 2015;24(9):1951-1958.
28. Jin L, Balian G, Li XJ. Animal models for disc degeneration-an update. *Histol Histopathol*. 2018;33(6):543-554.
29. Alini M, Eisenstein SM, Ito K, et al. Are animal models useful for studying human disc disorders/degeneration? *Eur Spine J*. 2008;17(1):2-19.
30. Wei F, Zhong R, Pan X, et al. Computed tomography-guided sub-endplate injection of pingyangmycin for a novel rabbit model of slowly progressive disc degeneration. *Spine J*. 2019;19(2):e6-e18.
31. Wei F, Zhong R, Wang L, et al. Pingyangmycin-induced in vivo lumbar disc degeneration model of rhesus monkeys. *Spine (Phila pa 1976)*. 2015;40(4):E199-E210.
32. Holm S, Holm AK, Ekström L, Karladani A, Hansson T. Experimental disc degeneration due to endplate injury. *J Spinal Disord Tech*. 2004;17(1):64-71.
33. Yin S, Du H, Zhao W, et al. Inhibition of both endplate nutritional pathways results in intervertebral disc degeneration in a goat model. *J Orthop Surg Res*. 2019;14(1):138.
34. Hutton WC, Murakami H, Li J, et al. The effect of blocking a nutritional pathway to the intervertebral disc in the dog model. *J Spinal Disord Tech*. 2004;17(1):53-63.
35. Sun Z, Zheng X, Li S, et al. Single impact injury of vertebral endplates without structural disruption, initiates disc degeneration through Piezo1 mediated inflammation and metabolism dysfunction. *Spine (Phila pa 1976)*. 2022;47(5):E203-e213.
36. Maroudas A, Stockwell RA, Nachemson A, Urban J. Factors involved in the nutrition of the human lumbar intervertebral disc: cellularity and diffusion of glucose in vitro. *J Anat*. 1975;120(Pt 1):113-130.
37. Boubriak OA, Watson N, Sivan SS, Stubbens N, Urban JP. Factors regulating viable cell density in the intervertebral disc: blood supply in relation to disc height. *J Anat*. 2013;222(3):341-348.
38. Lee JT, Cheung KM, Leung VY. Systematic study of cell isolation from bovine nucleus pulposus: improving cell yield and experiment reliability. *J Orthop Res*. 2015;33(12):1743-1755.
39. Duance VC, Crean JK, Sims TJ, et al. Changes in collagen cross-linking in degenerative disc disease and scoliosis. *Spine (Phila pa 1976)*. 1998;23(23):2545-2551.
40. Eyre D, Matsui Y, Wu J. Collagen polymorphisms of the intervertebral disc. *Biochem Soc Trans*. 2002;30:844-848.
41. Ricard-Blum S, Ruggiero F. The collagen superfamily: from the extracellular matrix to the cell membrane. *Pathol Biol (Paris)*. 2005;53(7):430-442.
42. Roberts S, Menage J, Urban JP. Biochemical and structural properties of the cartilage end-plate and its relation to the intervertebral disc. *Spine (Phila pa 1976)*. 1989;14(2):166-174.
43. Yu J, Tirlapur U, Fairbank J, et al. Microfibrils, elastin fibres and collagen fibres in the human intervertebral disc and bovine tail disc. *J Anat*. 2007;210(4):460-471.
44. Qu D, Subramony SD, Boskey AL, Pleshko N, Doty SB, Lu HH. Compositional mapping of the mature anterior cruciate ligament-to-bone insertion. *J Orthop Res*. 2017;35(11):2513-2523.
45. Schwartz AG, Pasteris JD, Genin GM, Daulton TL, Thomopoulos S. Mineral distributions at the developing tendon enthesis. *PLoS One*. 2012;7(11):e48630.
46. Khanarian NT, Boushell MK, Spalazzi JP, Pleshko N, Boskey AL, Lu HH. FTIR-I compositional mapping of the cartilage-to-bone interface as a function of tissue region and age. *J Bone Miner Res*. 2014;29(12):2643-2652.
47. Longley R, Ferreira AM, Gentile P. Recent approaches to the manufacturing of biomimetic multi-phasic scaffolds for Osteochondral regeneration. *Int J Mol Sci*. 2018;19(6):1755.
48. Wang F, Ying Z, Duan X, et al. Histomorphometric analysis of adult articular calcified cartilage zone. *J Struct Biol*. 2009;168(3):359-365.

49. Mansfield JC, Bell JS, Winlove CP. The micromechanics of the superficial zone of articular cartilage. *Osteoarthr Cartil.* 2015;23(10):1806-1816.
50. DiDomenico CD, Lintz M, Bonassar LJ. Molecular transport in articular cartilage - what have we learned from the past 50 years? *Nat Rev Rheumatol.* 2018;14(7):393-403.
51. Martin JT, Wesorick B, Oldweiler AB, Kosinski AS, Goode AP, DeFrate LE. In vivo fluid transport in human intervertebral discs varies by spinal level and disc region. *JOR Spine.* 2022;5(2):e1199.

**How to cite this article:** Li, Y.-H., Wu, H.-L., Li, Z., Li, B.-B., Zhu, M., Chen, D., Ye, F.-H., Yu, B.-S., & Huang, Y.-C. (2022). Species variation in the cartilaginous endplate of the lumbar intervertebral disc. *JOR Spine*, 5(3), e1218. <https://doi.org/10.1002/jsp2.1218>